04,06

# Synthesis, crystal structure, phase transitions and dielectric relaxation in $La^{3+}$ modified $Sr_{0.5}Ba_{0.5}Nb_2O_6$ ceramics

© N.V. Makinyan[1], A.L. Bulanova[2], A.A. Zabolotnyi[2], A.V. Pavlenko[1]

[1] Southern Scientific Center, Russian Academy of Sciences,
Rostov-on-Don, Russia
[2] Southern Federal University,
Rostov-on-Don, Russia

E-mail: norair.makinyan@yandex.ru

*Received July 10, 2025*
*Revised July 18, 2025*
*Accepted July 19, 2025*

The crystal structure, dielectric and ferroelectric characteristics of $Sr_{0.5}Ba_{0.5}Nb_2O_6$ ceramics modified at the synthesis stage beyond the stoichiometry of 1 wt.% (weight percent) $La_2O_3$ (SBN50-La) have been studied. It is shown that ceramics are pure, $La^{3+}$ cations are embedded in A1 positions, and the parameters of the tetragonal unit cell are $a = 12.4800$ Å, $c = 3.9354$ Å. Analysis of the $\varepsilon'(T, f)$ and $\varepsilon''(T, f)$ dependences revealed that SBN50-La is a relaxor ferroelectric. It is shown that the dielectric response of SBN50-La ceramics at $T = 83-493$ K and $f = 20-10^6$ Hz has a contribution from three relaxation processes. The mechanisms of these processes are discussed.

**Keywords:** strontium barium niobate, dielectric characteristics, relaxor ferroelectric, dielectric relaxation.

DOI: 10.61011/PSS.2025.08.62257.183-25

## 1. Introduction

Presently, ferroelectric materials are widely applied in many fields of engineering [1,2]. A common and effective practice of intentional improvement of ferroelectric materials properties is their doping, i. e. incorporation of, for example, rare earth elements ($Y^{3+}$, $La^{3+}$, $Ce^{3+}$ and so on) into the structure. It often results in improvement of such characteristics as permittivity, residual polarization, a pyroelectric coefficient, etc. [3,4]. Besides, in some cases, doping facilitates optimization of technological processes during synthesis of samples [5]. Strontium and barium niobates $(Sr,Ba)Nb_2O_6$ (SBN) stand out among ferroelectrics with a structure of tetragonal tungsten bronze (TTB), since they have high values of permittivity (in crystals it can be up to $\sim 80000$ in the phase transition region [6,7]) and the pyroelectric coefficient ($0.06\,\mu C/cm^2/K$ [8]), thereby making them in demand for application in nonlinear optics and infrared radiation sensors [9,10]. They are comprehensively studied by various research teams in a pure form [11–13] and in the form of single crystals and ceramics doped with rare earth elements [5,14–24]. It has been multiply noted that incorporation of a dopant allows significantly changing a temperature of the phase transition from a ferroelectric into a paraelectric phase and electrophysical parameters of the material thereby. Fundamentally, a system of the SBN solid solutions is interesting in terms of having a concentration transition into a relaxor state, thereby affecting the parameters of the material and its domain structure. Since SBNs are unoccupied TTBs, a material production technology, synthesis regulations and various additives (to be incorporated both stoichiometrically and superstoichiometrically) can significantly affect the properties of the materials, which shall undoubtedly be taken into account. Physical material science uses a colossally wide spectrum of oxides and carbonates as modifiers. The influence of some of them primarily reduces to embedding of certain cations into a basic structure, while the others ($Li_2CO_3$, $MnO_2$, $La_2O_3$, $B_2O_3$) also act as a source of „a liquid phase“, which can positively affect ceramic properties of the material (to improve homogeneity, density, strength of the ceramic), which is especially important when using the ceramic as a target in installations for producing films by plasma methods. It is known presence of target heterogeneities and their low density have a negative effect. Regarding SBN, one of the most interesting modifiers is lanthanum oxide [20–24]. It was multiply noted in studies by E.G. Kostsov [9,25] that incorporation of $La_2O_3$ at the stage of production of the SBN50 ceramic to be used for producing SBN50 thin films in the future allows increasing a pyrocoefficient and some other properties in 1.5–2 times. Taking into account that it is still unclear how modifying with lanthanum oxide affects the structure, the dielectric and ferroelectric properties of the SBN50 ceramic, it is believed that the studies are relevant in this field and the present study is dedicated to it.

## 2. Objects. Manufacturing and research methods

The $Sr_{0.5}Ba_{0.5}Nb_2O_6$ ceramic that is superstoichiometrically modified by $La_2O_3$ (1 wt.%) (i. e. the modifier

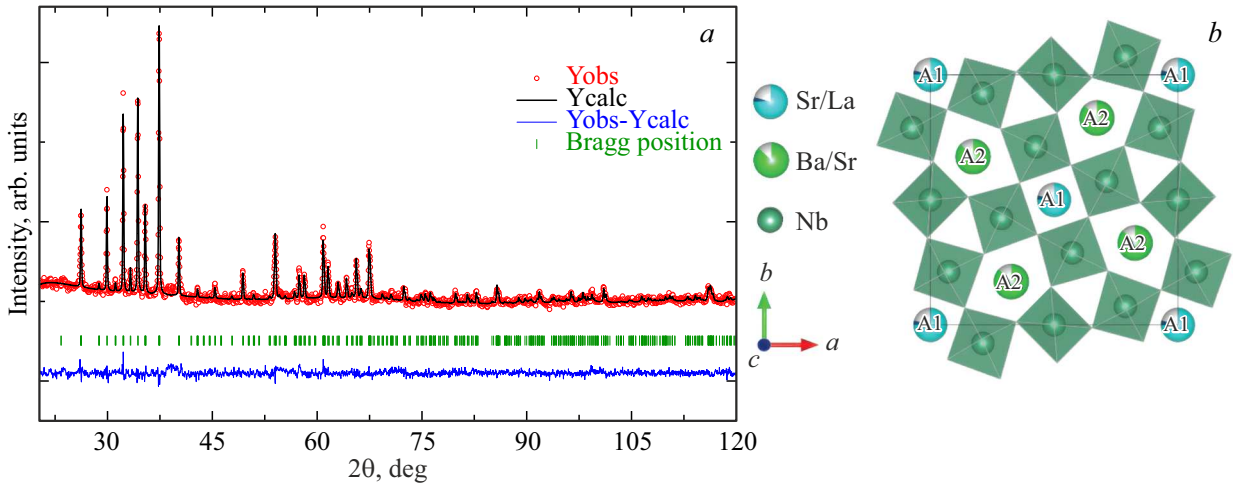


**Figure 1.** X-ray diffraction data (Yobs) and the diffraction model calculated by the Rietveld method (Ycalc) for the SBN50-La ceramic ($a$); the schematic image of the crystal structure of the SBN50-La compound ($b$).

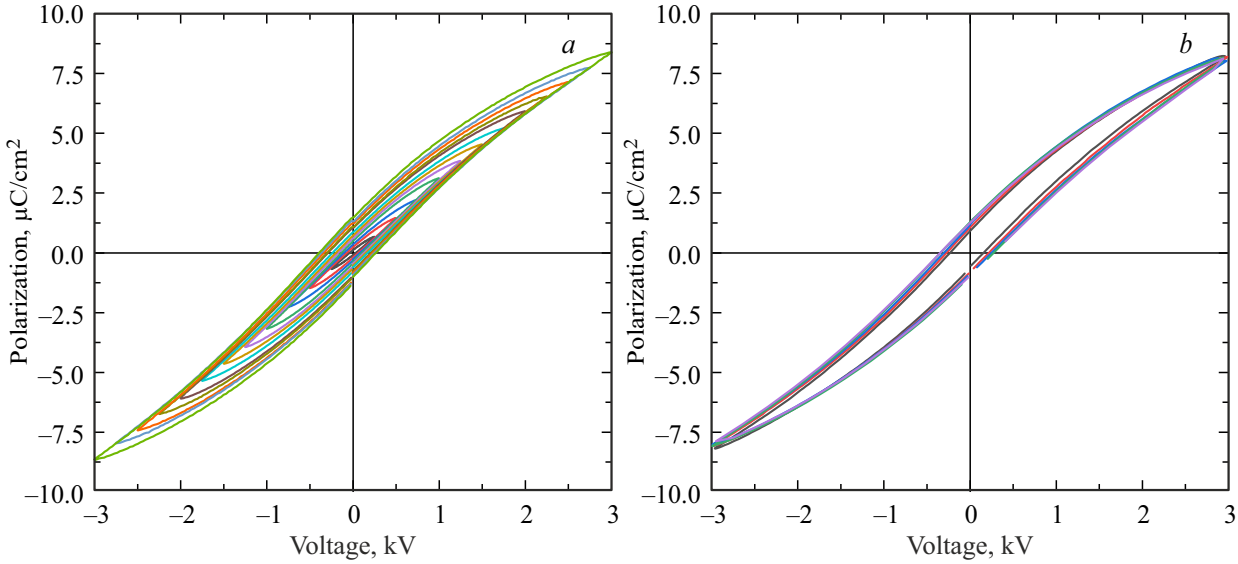


**Figure 2.** Dependences $P(U, f = 200\,\text{Hz})$ of the SBN50-La ceramic at the various amplitudes of $U$ ($a$); the dependences of $P(U)$ of the SBN50-La ceramic at $f = 10-1000\,\text{Hz}$ ($b$).

was incorporated above a stoichiometry of the initial composition) was synthesized in a two-stage solid-phase method. Initial reagents were powders $SrCO_3$ (99.9 %), $BaCO_3$ (99.9 %), $Nb_2O_5$ (99 %) and $La_2O_3$ (99 %) that were pre-dried at 773 K for 3 h. The powders of the pre-weighed initial reagents were thoroughly ground and mixed in an agate mortar with addition of ethanol for 30 min. Then the produced blend was calcinated in a corundum in air at the temperature of 1173 K for 6 h to decompose carbonates and to bind precursors as intermediate phases, the heating rate was 4 K/min. After that, the samples were cooled down to the room temperature at a furnace cooldown temperature. The produced powders were homogenized to homogeneity with addition of polyvinyl alcohol (5 %) for 30 min, pressed into discs of the diameter of 12 mm at the pressure of 9 MPa and sintered at the temperature of 1623 K for 4 h.

Powder X-ray data were collected using the DRON-3M diffractometer with an installed Fe filter of Co$K_\alpha$ radiation at a rate of $2^\circ(2\theta)$/min. To refine the crystal structure using the Rietveld method, XRD data were used in the angle range $15^\circ \le 2\theta \le 120^\circ$ with a step of $0.03^\circ$ and an exposure at each point of 3 s. The data were analyzed in the Jana 2006 program [26]. Data for $Sr_{0.48}Ba_{0.52}Nb_2O_6$ (a space group P4bm) [13] were used as an initial model to refine the crystal structure.

In order to carry out electrophysical measurements, electrodes were applied to the produced samples using silver-containing paste. Relative complex permittivity $\varepsilon^* = \varepsilon' - i\varepsilon''$ ($\varepsilon'$ and $\varepsilon''$ are a real and an imaginary

part of $\varepsilon^*$, respectively) was measured within the temperature range $T = 83-493$ K and the frequency range $f = 20-10^6$ Hz using a cryosystem Linkam THMS600 stage and a broadband LCR analyzer E7-28.

A measurement complex based on a ferroelectric analyzer DX-FE2000, a thermal chamber DXSC-2 and a laser vibration meter DXLV-03 was used to obtain loops of dielectric $(P(U))$ and mechanical $(D(U))$ hysteresis within the temperature range $T = 293-473$ K at the frequency of 10 Hz (the signal shape is triangular) at the values of externa electric voltage $U = 0 \pm 4$ kV as well as volt-farad dependences $(C(U))$ at the frequency and the amplitude of the measurement signal, 10 kHz and 15 V, respectively. The fatigue effects were studied after impact of sawtooth pulses of the frequency and the amplitude of, 1 kHz and 2500 V, respectively. The values of residual and maximum polarizations ($P_r$ and $P_{\max}$) and the coercive field ($E_c$) of the samples were calculated using the analyzer software. The pyroelectric current was measured in a dynamic mode in a bench that included a thermal table (Dexinmag) and an electrometer Keithley 6514. The current was recorded at a linear increase of the temperature at the rate of 5 K/min within the interval $T = 308-473$ K.

## 3. Experimental results and discussion

A diffraction profile of the sample (Figure 1) is typical for the SBM family with the TTB structure [13]. In order to confirm formation of the TTB phase with the space group P4bm and to calculate parameters of the lattice cell, the structure was refined by the Rietveld method. It is indicated in some studies that rare earth element are most often prone to occupy exactly tetragonal channels A1, while their presence in the structure significantly affects not only crystallographic parameters, but electrophysical properties as well [24,27–29].

In this case, in our used model the $La^{3+}$ ions were refined in the position 2a. It is clear from the refinement results (Figure 1) that superstoichiometric incorporation of $La_2O_3$ in the amount of 1 wt.% results in variation of the lattice cell parameter as compared to pure SBN50 [28,30] $a = 12.4800$ Å, $c = 3.9354$ Å, thereby confirming partial embedment of the $La^{3+}$ cations into the basic structure. Besides, we were able to refine occupancy of the La atoms in the position 2a. Table shows the crystallographic parameters for the SBN50-La ceramic.

As can be seen in Figure 2, at the room temperature the SBN50-La ceramic is in a polar phase — under field effect there is a family of expanding and amplitude-increasing loops of $P(U)$. Unlike the pure SBN50 ceramic, the loops of $P(U)$ for SBN50-La are more elongated in a form and they can not be fully saturated in the fields $U \sim 3$ kV (at this $U$ the SBN50-La ceramic is characterized by the following values $E_c = 21$ kV/cm, $P_r = 1.52\,\mu$C/cm$^2$ and $P_{\max} = 8.71\,\mu$C/cm$^2$, respectively).

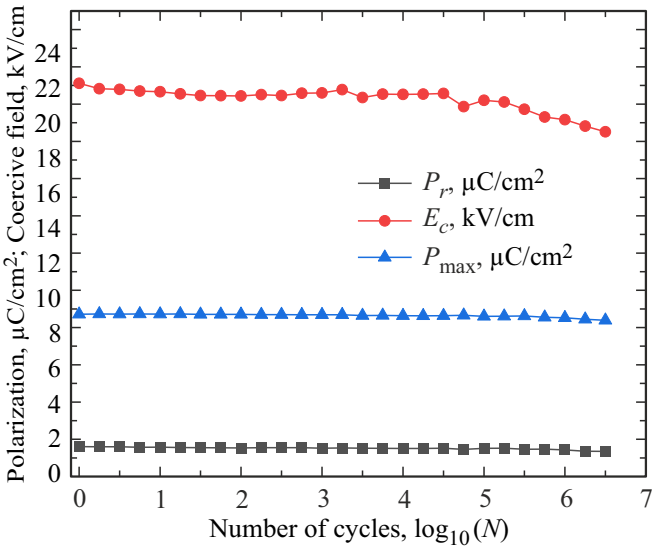


**Figure 3.** Dependences $P_r, E_c$ and $P_{\max}$ of the SBN50-La ceramic on the number of switching cycles.

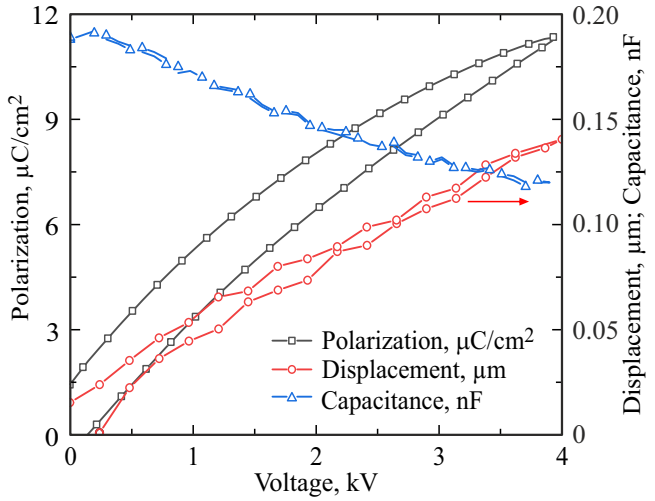


**Figure 4.** Loops of $P(U)$ and $D(U)$ of the SBN50-La ceramic.

Variation of the external field frequency from 10 to 1000 Hz almost did not result in changes of the loop parameters (Figure 2, *b*). It is found when analyzing fatigue effects manifested in the ferroelectrics during multiple switching of polarization that up to $10^6$ switching cycles polarization characteristics of the SBN50-La ceramic are almost unchanged and further on slight reduction of the main characteristics is recorded due to heating of the sample during multiple cycling (Figure 3). By taking into account that in the SBN50-La ceramic studied by us stability of $P_r, E_c$ and $P_{\max}$ was either comparable [31] or better [32] to/than the pure SBN-50 ceramic, it can be concluded that incorporated lanthanum oxide positively affects the ferroelectric characteristics of the material. This is also confirmed by results of measurements of the dependences

Coordinates of the atoms and isotropic thermal shifts for the ceramic $Sr_{0.5}Ba_{0.5}Nb_2O_6 + 1$ wt.% $La_2O_3$

| Atom | Wyckoff position | $x/a$ | $y/b$ | $z/c$ | $B_{iso}$, Å$^2$ | Site occ. |
|---|---|---|---|---|---|---|
| Ba2 | 4c | 0.1728(4) | 0.6728(4) | 0.4927(19) | 2.38(21) | 0.3125 |
| Sr2 | 4c | 0.1728(4) | 0.6728(4) | 0.4927(19) | 2.38(21) | 0.125 |
| Sr1 | 2a | 0 | 0 | 0.4892 | 1 | 0.1875 |
| La1 | 2a | 0 | 0 | 0.4892 | 1 | 0.0106(24) |
| Nb1 | 2b | 0.5 | 0 | 0.016 | 0.57(20) | 0.25 |
| Nb2 | 8d | 0.0741(4) | 0.2122(4) | 0 | 0.19(13) | 1 |
| O1 | 4c | 0.283(2) | 0.783(2) | 1.01(6) | 1.5 | 0.5 |
| O2 | 8d | 0.139(2) | 0.068(3) | 0.959(18) | 1.5 | 1 |
| O3 | 8d | 0.9876(16) | 0.347(4) | 1.058(16) | 1.5 | 1 |
| O4 | 2b | 0.5 | 0 | 0.52(7) | 1.5 | 0.25 |
| O5 | 8d | 0.057(3) | 0.207(2) | 0.50(6) | 1.5 | 1 |

SG: P4bm, $a = 12.4800$ Å, $c = 3.9354$ Å, $R_p = 2.02\,\%$, $R_{wp} = 2.62\,\%$ and $\chi^2 = 0.87$

$C(U)$ and $D(U)$ of the samples (Figure 4): when applying $U = 0{-}4$ kV capacitance of the sample is reduced by 39 %, while the maximum mechanical deformation of the sample was $0.140\,\mu$m ($\sim 0.018\,\%$). No significant difference is detected in the dependences $C(U)$ and $D(U)$ that were measured before and after the experiment of analysis of the fatigue effects.

In order to determine temperatures of the phase transformations in the SBN50-La ceramic, we have performed a set of complementary studies, which included measurements of the dependences $P(U, T)$, $\varepsilon'(T, f)$ and $\varepsilon''(T, f)$ as well as the pyroelectric current $I(T)$ in the dynamic mode (for the pre-polarized sample). As can be seen from Figure 5, the increase of the temperature from 303−473 K results in narrowing and an amplitude-decrease of the loop of $P(U)$ of the ceramic, while the magnitudes $P_r$, $E_c$ and $P_{\max}$ decrease in the sharpest way within the interval $T = 303{-}363$ K, and when $T > 363$ K a rate of their decrease is reduced (this is most clearly seen for the case of $P_r(T)$) (Figure 5, the insert).

It is undoubtedly related to a smeared phase transition from the ferroelectric into the paraelectric phase. This is confirmed by the dependences $\varepsilon'(T, f)$ and $\varepsilon''(T, f)$ of the sample, which are shown in Figure 6.

As the temperature decreases within the interval $T = 360{-}493$ K relative permittivity of the SBN50-La ceramic varies according to the Curie-Weiss law ($\varepsilon' = C/(T - T_C)$ almost at all the frequencies, where $C$ — the Curie constant depending on a material, $T_C$ — the Curie temperature), which is typical for the ferroelectric materials in the paraelectric phase. When $T < 360$ K, further decrease of the temperature first results in origination of dispersion $\varepsilon'$ and $\varepsilon''$ and then maximums ($T_{m1}$) are formed within the interval $T = 288{-}320$ K and they are shifted into the low temperature and increase in magnitude as $f$ decreases. The dependence $T_{m1}(f)$ (Figure 6, *c*) within the frequency range $f = 20{-}10^6$ Hz was well described by the Vogel-Fulcher relationship $f = f_0 \exp\left(E_{\text{act}}/(k(T_m - T_f))\right)$ ($f_0 = 6 \cdot 10^{10}$ Hz — the frequency of attempts of overcoming a potential barrier $E_{\text{act}} = 0.064$ eV, $k$ — the Boltzmann constant, $T_f = 251$ K — the Vogel-Fulcher temperature). With further decrease of the temperature there is generally monotonic decrease of $\varepsilon'$, but „humps“ are recorded around 200 K at the frequencies below 105 Hz. Patterns with similar behavior were also observed at the dependences $\varepsilon''(T, f)$, but anomalies in the low-temperature range were well pronounced and were frequency-dependent maximums. We note that the temperature hysteresis on the curves $\varepsilon'(T)$ and $\varepsilon''(T)$ was recorded only when $T = 123{-}373$ K, while the values of $T_{m1}$ for the mode of heating and cooling differed and also depended on the frequency — for $f = 20$ Hz shifts were $\Delta T \sim 17$ K, and for $f = 1$ MHz they were $\Delta T \sim 8.4$ K.

The obtained results indicate that in terms of a nature of manifestation of the ferroelectric properties the studied SBN50-La ceramic belongs to ferroelectric-relaxors (FER), while embedment of the $La^{3+}$ cations into the basic structure significantly enhanced manifestation of the relaxor properties. The Burns temperature that corresponds to a temperature, at which the FERs originate polar regions, is 360 K, as can be seen in Figure 6. The relaxor state in multi-component ferroelectrics is related to fluctuations of a chemical composition across a material volume due to disordered atom arrangement in respective structure positions. In case of the studied sample, the SBN solid solutions are characterized by disordered arrangement of

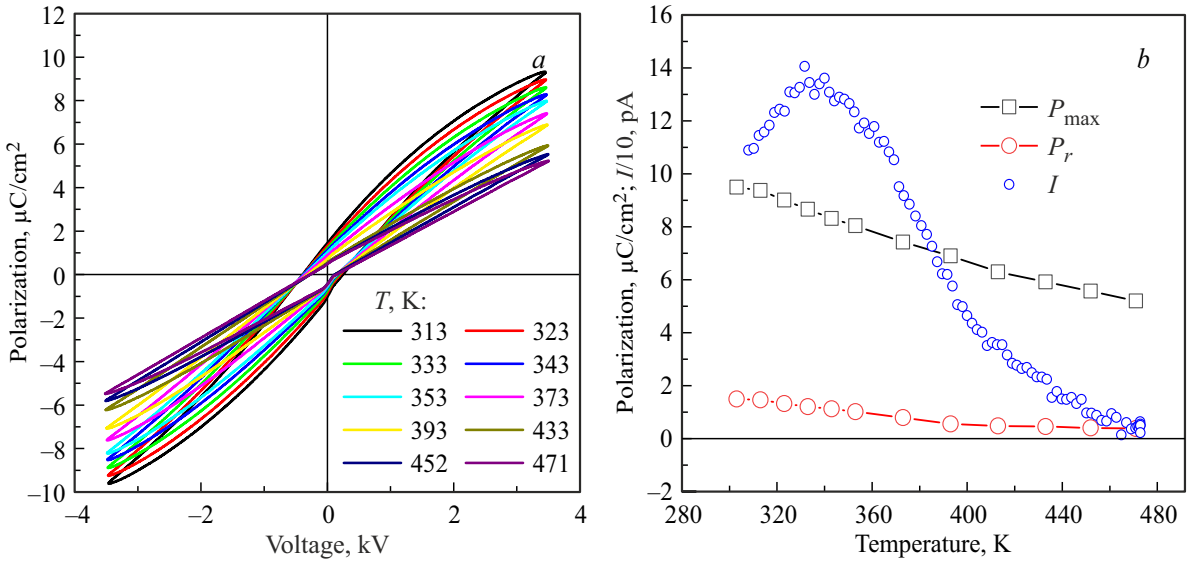


**Figure 5.** Dependences $P(U)$ of the SBN50-La ceramic at the different temperatures at the frequency of 200 Hz ($a$); the dependences of calculated $P_r$, $P_{max}$ and the pyroelectric current $I$ on the temperature ($b$).

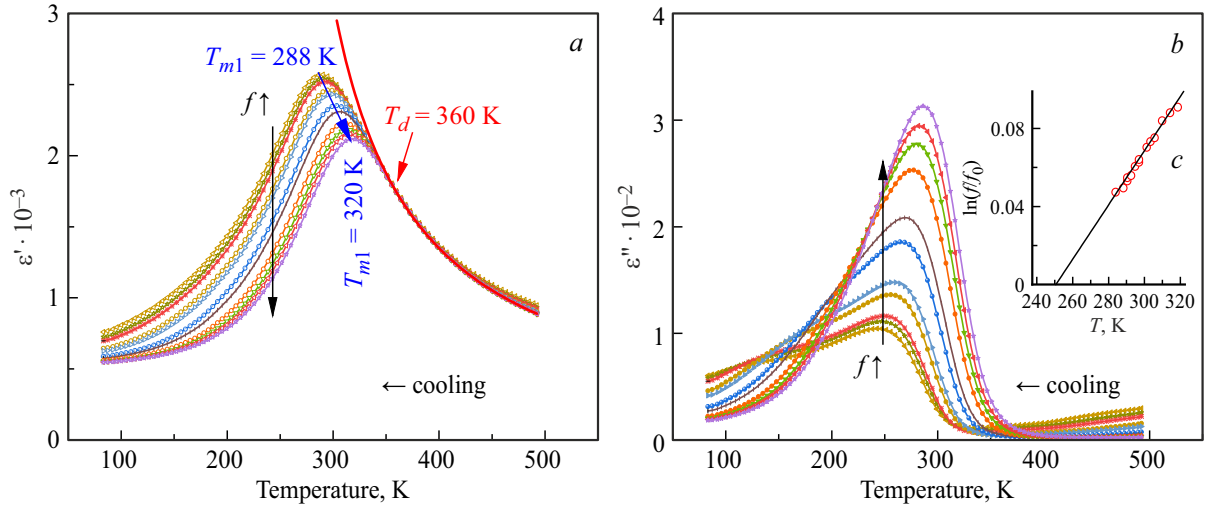


**Figure 6.** Dependences of $\varepsilon'(T, f)$ and $\varepsilon''(T, f)$ of the SBN50-La ceramic within the interval $T = 83-493$ K at the frequencies $f = 200-10^6$ Hz ($a$ and $b$). The red solid lines illustrate the fulfillment of the Curie-Weiss law. The insert illustrates the fulfillment of the Vogel-Fulcher law for the dependence $T_{m1}(f)$ ($c$).

the cations $Ba^{2+}$ and $Sr^{2+}$ in the TTB structure. Only the $Sr^{2+}$ ions are localized in the tetragonal positions A1, while the cations $Ba^{2+}$ and $Sr^{2+}$ are statistically distributed in the pentagonal positions A2. It should be also noted that both the positions are only partially occupied [33]).

The polar behavior varies from the usual ferroelectric to the relaxor-like one at the ratio $Sr^{2+}/Ba^{2+} > 0.5$ [34], but a physical mechanism responsible for this crossover is still unclear. It is believed that as soon as only a half of the $Sr^{2+}$ cations occupy the positions A2, then „crossover" occurs. Occupancy of the positions A1 and A2 with the cations $Ba^{2+}$ and $Sr^{2+}$ can be affected both by varying the sample production conditions (annealing times and temperatures, etc.) as well as by incorporating various additives [30], which is most likely observed by us. It can also result in inducibility of the polar regions under effect of the electric field on the material, with their subsequent existability at the temperatures that significantly exceed $T_{m1}$. It is for this reason we have recorded the loops of $P(U)$ up to 473 K as well as a pyroelectric response in the SBN50-La ceramic that is pre-polarized with the constant electric field (Figure 5, $b$).

Let us consider evolution of dispersion $\varepsilon''$ and $\varepsilon'$ of the materials in more detail. On the Cole–Cole diagrams (the dependences $\varepsilon''(\varepsilon')$) of the SBN50-La ceramic (Figure 7), we first observed one arc of a semicircle $R_1$ ($T = 373-473$ K), then, when $T$ is from 303 K to 373 K — two frequency-separated arcs of the semicircles $R_1$ and R

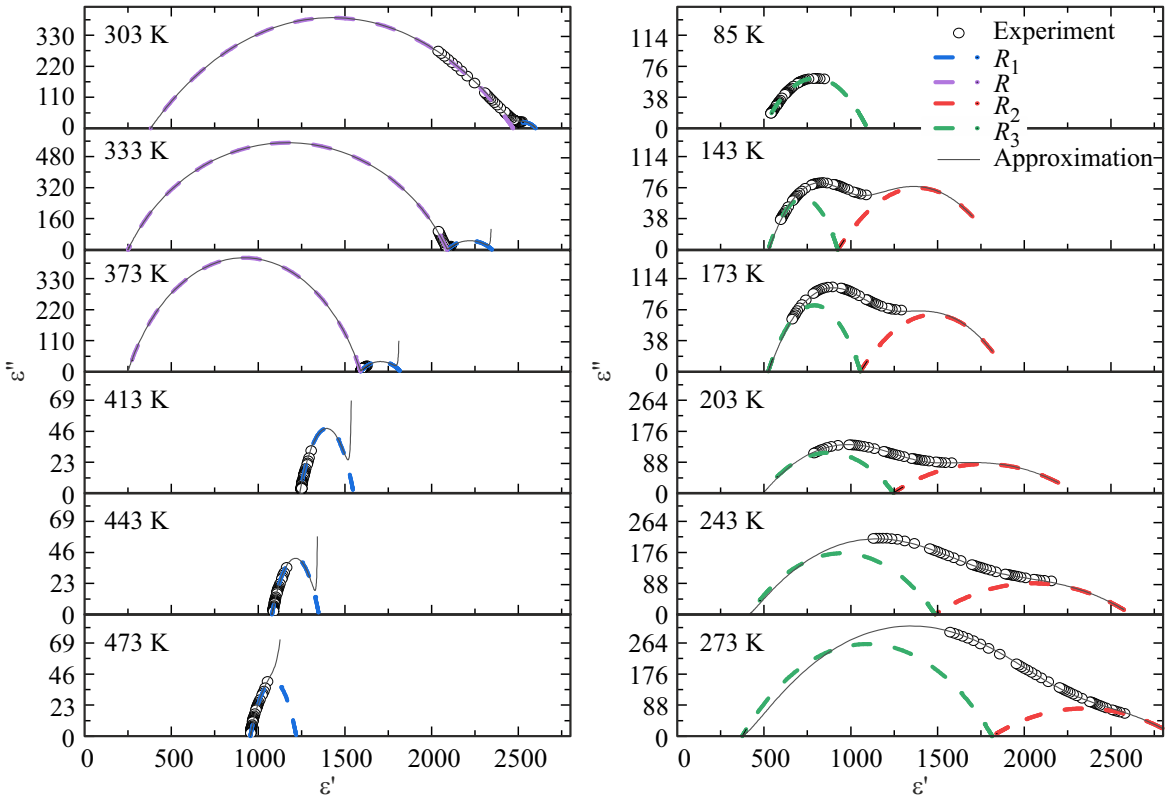


**Figure 7.** Experimental (light markers) and theoretical (lines) dependences of $\varepsilon''(\varepsilon')$ of the SBN50-La ceramic at the temperatures 85–473 K.

(the boundary $f$ decreases with decrease of $T$), and when $T < 303$ K — the arc $R_1$ almost disappears, and R becomes a two-component one $R_2$ and $R_3$. It indicates that within the temperature range $T = 83-493$ K and $f = 20-10^6$ Hz the dielectric response of the SBN50-La ceramic is contributed by three relaxation processes. Various models that differ by a form of relaxor distribution function were considered for approximation of the experimental dependences $\varepsilon''(\varepsilon')$, $\varepsilon''(f)$ and $\varepsilon'(f)$ [35]. However, the best results were achieved when using the following relationship, in which a contribution by each process of dielectric relaxation was described by a symmetric Cole-Cole function of relaxation time distribution:

$$\varepsilon^* = \varepsilon' + i \cdot \varepsilon'' = \varepsilon_{\infty 1} + \frac{\varepsilon_{S1} - \varepsilon_{\infty 1}}{1 + (i \cdot f \cdot \tau_1)^{1-\alpha_1}} + \frac{\varepsilon_{S2} - \varepsilon_{S1}}{1 + (i \cdot f \cdot \tau_2)^{1-\alpha_2}} + \frac{\gamma_{st}}{2\pi \cdot f \cdot \varepsilon_0}, \qquad (1)$$

where $\alpha_1$ and $\alpha_2$ — coefficients that characterize relaxation time distributions (from 0 to 1); $\varepsilon_{s1}$, $\varepsilon_{s2}$ and $\varepsilon_{\infty 1}$ — static and high-frequency permittivities; $\tau_1$ and $\tau_2$ — the relaxation times; $\varepsilon_0$ — the dielectric constant; $\gamma_{st}$ — through conductivity. The contribution by a singular term shall have been taken into account only at the maximum temperatures. The results of approximation are shown in Figure 7, *a*, while the dependences of the fitting parameters on the temperature are shown in Figure 8.

By taking into account the temperature ranges, at which we observe each of the relaxation processes, the dependences of their parameters on the temperature as well as results of the studies [36,37], the following conclusions can be made. The relaxation process $R_1$ that occurs in the paraelectric phase when $T > T_d$, whose description required taking into account the contribution by $\gamma_{st}$, while $\alpha_1$ and $\Delta\varepsilon$ do not depend on the temperature, can be related to manifestation of Maxwell-Wagner polarization, which is often manifested in the ceramics. The main cause is accumulation of a charge, during increase of their conductivity, on grain boundaries or in near-electrode regions due to differences of dielectric properties of a grain bulk and a grain boundary [35].

When $T < T_d$, the dielectric response is mainly contributed by the relaxation processes $R_2$ and $R_3$. The relaxation $R_2$ is the strongest around $T_m$ (Figure 8, *a*), and as the temperature decreases, it is „decelerated“ from $f \sim 10^9$ to $\sim 10^2$ Hz against the background of increase of $\alpha$ from 0.3 to 0.72. The relaxation $R_3$ lower-frequential and less strong around $T_m$, but with decrease of the temperature, it is decelerated from $f \sim 10^4$ Hz to $\sim 10^{-2}$ Hz and starts making a contribution to the dielectric response, which is comparable to $R_2$. Taking into account the studies [36,37], both the detected relaxation processes are related to polar fluctuations in the SBN50-La ceramic and most likely caused by switching ($R_2$) and an oscillation ($R_3$) of polar

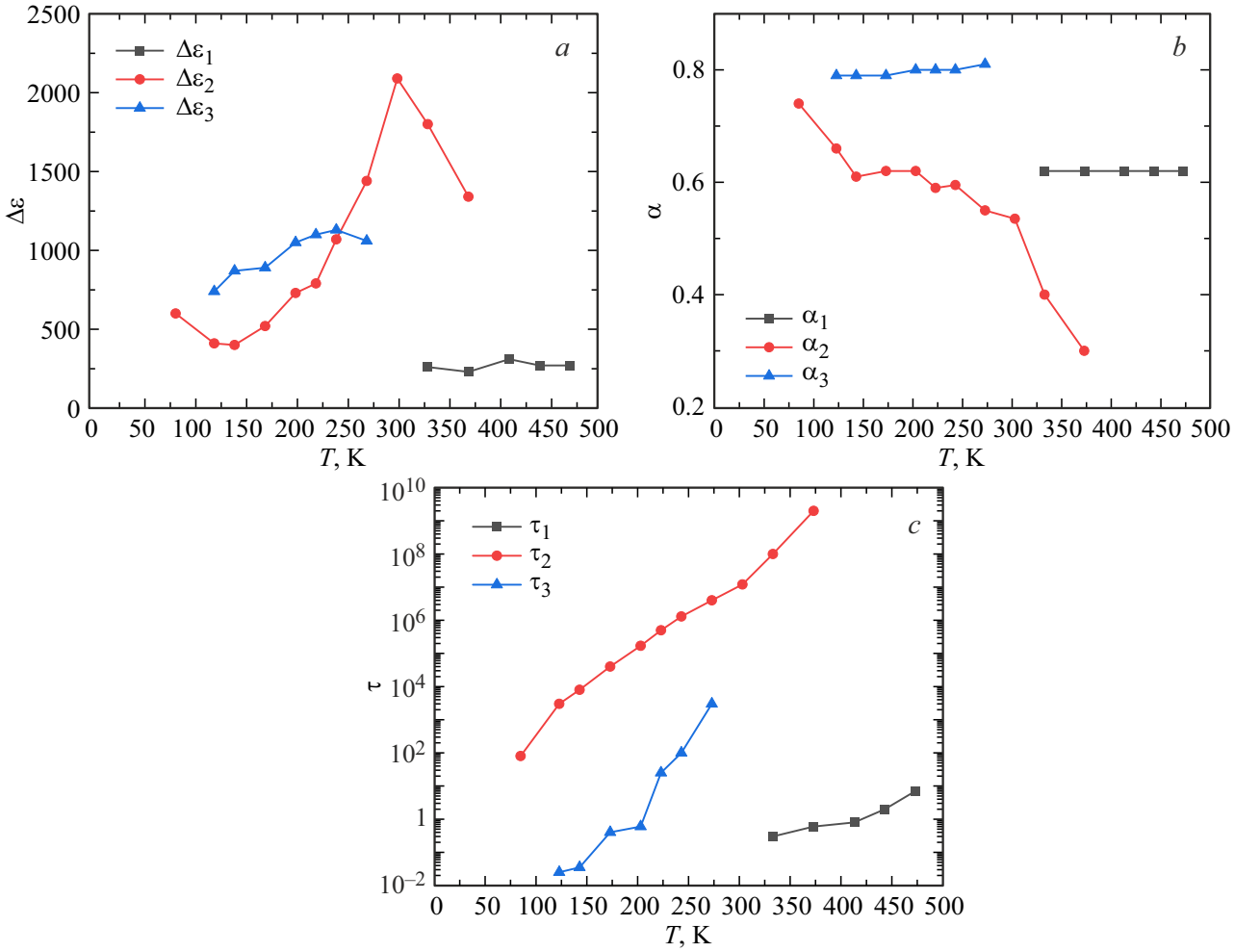


**Figure 8.** Temperature dependences of the parameters $\Delta\varepsilon = \varepsilon_s - \varepsilon_\infty$, $\alpha$ and $\tau$ which are obtained when approximating the dependences $\varepsilon''(\varepsilon')$ using (1).

nanodomains. We note that the contribution by oscillations of the domain walls in SBN is manifested when $T < T_d$ at the frequency $\sim 10^{10}$ Hz [36], whence we do not observe it in our experiment.

## 4. Findings and conclusion

Thus, the study provides the results of complex studies of the properties of the $Sr_{0.5}Ba_{0.5}Nb_2O_6$ ceramic that is superstoichiometrically modified at the synthesis stage with 1 wt.% $La_2O_3$. It is found that this modification results in variation of the lattice cell parameters of the material relative to pure $Sr_{0.5}Ba_{0.5}Nb_2O_6$ and is induced by embedment of the $La^{3+}$ cations into the tetragonal channels that are initially occupied only by $Sr^{2+}$. It results in the fact that the material in the produced ceramic exhibits, on the one hand, enhancement of the relaxor properties and, on the other hand, improvement of the ferroelectric characteristics.

Dispersion $\varepsilon'$ and $\varepsilon''$ of the SBN50-La ceramic when $T = 83-493$ K and $f = 20-10^6$ Hz was analyzed to show that the in the dielectric response of the material within the frequency range $f = 20-10^6$ Hz there were recorded contributions by the three relaxation processes, and two of them are related to the paraelectric subsystem, and one is related to polarization of the Maxwell-Wagner type. It is important to note that the dielectric response that is close by the type was detected only in the SBN81 single crystal and was not observed in SBN61 and SBN50 [36]. These results indicate that incorporation of the $La^{3+}$ cations even at such small concentrations significantly affect the crystal structure and properties of strontium barium niobates, and it is reasonable to take this into account when producing ceramics of these materials.

### Acknowledgments

The authors would like to thank Joint Scientific and Technological Equipment Center of the Southern Scientific Center of the Russian Academy of Sciences (Research,

Development, Testing) for provided equipment for the studies.

### Funding

The study was supported by the Ministry of Science and Higher Education of the Russian Federation within the framework of state assignment projects of the Southern Scientific Center of the Russian Academy of Sciences (state registration No. 125011400232-3).

### Conflict of interest

The authors declare that they have no conflict of interest.

## References

[1] M.E. Lines, A.M. Glass. Principles and applications of ferroelectrics and related materials. Oxford university press, 2001.
[2] A.K. Bain, P. Chand. Ferroelectrics: Principles and applications, John Wiley & Sons, Inc. (2017).
[3] Y. Chen, D. Zhang, Z. Peng, M. Yuan, X. Ji. Front. Mater. **8**, *7*, 1 (2021).
[4] T. Bian, T. Zhou, Y. Zhang. Energies **15**, *22*, 8442 (2022).
[5] R.B. Maciolek, S.T. Liu. J. Electron. Mater. **4**, *3*, 517 (1975).
[6] A.M. Glass. J. Appl. Phys. **40**, *12*, 4699 (1969).
[7] T. Lukasiewicz, M.A. Swirkowicz, J. Dec, W. Hofman, W. Szyrski. J. Cryst. Growth **310**, *7–9*, 1464 (2008).
[8] A.M. Glass. Appl. Phys. Lett. **13**, *4*, 147 (1968).
[9] S. Ivanov, E.G. Kostsov. IEEE Sens. J. **20**, *16*, 9011 (2020).
[10] S. Gupta, S. Sharma, T. Ahmad, A.S. Kaushik, P.K. Jha, V. Gupta, M. Tomar. Mater. Chem. Phys. **262**, 124300 (2021).
[11] P.B. Jamieson, S.C. Abrahams, J.L. Bernstein. J. Chem. Phys. **48**, *11*, 5048 (1968).
[12] T.S. Chernaya, B.A. Maksimov, T.R. Volk, L.I. Ivleva, V.I. Simonov. FTT **42**, *9*, 1668 (2000). (in Russian).
[13] S. Podlozhenov, H.A. Graetsch, J. Schneider, M. Ulex, M. Wöhlecke, K. Betzler. Acta Crystallogr. Sect. B Struct. Sci. **62**, *6*, 960 (2006).
[14] S.T. Liu, A.S. Bhalla. Ferroelectrics **51**, *1*, 47 (1983).
[15] M. Said, T.S. Velayutham, W.H. Abd Majid. Ceram. Int. **43**, *13*, 9783 (2017).
[16] Y. Li, J. Liu, Y. Zhang, Y. Zhou, J. Li, W. Su, J. Zhai, H. Wang, C. Wang. Ceram. Int. **42**, *1*, 1128 (2016).
[17] S.T. Liu, R.B. Maciolek, J.D. Zook, B. Rajagopalan. Ferroelectrics **87**, *1*, 265 (1988).
[18] K. Buse, R. Pankrath, E. Krätzig. Opt. Lett. **19**, *4*, 260 (1994).
[19] M.-H. Li, T.-C. Chong, X.-W. Xu, H. Kumagai. J. Cryst. Growth **225**, *2–4*, 479 (2001).
[20] K. Umakantham, S.N. Murty, K. Sambasiva Rao, A. Bhanumathi. J. Mater. Sci. Lett. **6**, *5*, 565 (1987).
[21] J. Portelles, I. Gonzalez, A. Kiriev, F. Calderon, S. Garcia, N. Calzada. J. Mater. Sci. Lett. **12**, *23*, 1871 (1993).
[22] H. Amorín, F. Guerrero, J. Portelles, I. González, A. Fundora, J. Siqueiros, J. Valenzuela. Solid State Commun. **106**, *8*, 555 (1998).
[23] I.A. Santos, D. Garcia, J.A. Eiras. Ferroelectrics **257**, *1*, 105 (2001).
[24] Y. Yao, C.L. Mak, K.H. Wong, S. Lu, Z. Xu. Int. J. Appl. Ceram. Technol. **6**, *6*, 671 (2009).
[25] E.G. Kostsov. Ferroelectrics **314**, *1*, 169 (2005).
[26] V. Petříček, M. Duşek, L. Palatinus. Zeitschrift Für Krist. — Cryst. Mater. **229**, *5*, 345 (2014).
[27] T.R. Volk, V.Yu. Salobutin, L.I. Ivleva, N.M. Polozkov, R. Pankra, M. Veleke. FTT **42**, *11*, 2066 (2000). (in Russian).
[28] T.S. Velayutham, N.I.F. Salim, W.C. Gan, W.H. Abd. Majid. J. Alloys Compd. **666**, 334 (2016).
[29] L. Wei, Z. Yang, X. Chao, H. Jiao. Ceram. Int. **40**, *4*, 5447 (2014).
[30] M. Said, T.S. Velayutham, W.C. Gan, W.H. Abd Majid. Ceram. Int. **41**, *5*, 7119 (2015).
[31] M.A. Mohiddon, K.L. Yadav. J. Phys. D. Appl. Phys. **41**, *22*, 225406 (2008).
[32] P.K. Patro, A.R. Kulkarni, S.M. Gupta, C.S. Harendranath. Phys. B Condens. Matter **400**, *1–2*, 237 (2007).
[33] Yu.S. Kuz'minov. Segnetoelektricheskie kristally dlya upravleniya lazernym izlucheniem. Nauka, Moskva, (1982) (in Russian).
[34] H. Liu, B. Dkhil. J. Alloys Compd. **929**, 167314 (2022).
[35] A.S. Bogatin, A.V. Turik. Protsessy relaksatsionnoi polyarizatsii v dielektrikakh s bol'shoi skvoznoi elektroprovodnost'yu. Feniks, Rostov-na-Donu (2013) (in Russian).
[36] E. Buixaderas, C. Kadlec, M. Kempa, V. Bovtun, M. Savinov, P. Bednyakov, J. Hlinka. J. Dec. Sci. Rep. **7**, *1*, 18034 (2017).
[37] J. Dec, W. Kleemann, V.V. Shvartsman, D.C. Lupascu, T. Łukasiewicz. Appl. Phys. Lett. **100**, *5*, (2012).

*Translated by M.Shevelev*